THIRD EUROPEAN ROTORCRAFT AND POWERED LIFT AIRCRAFT FORUM

Paper No 41

# A NEW AIRFOIL FAMILY FOR ROTOR BLADES

MM. J.J. THIBERT, J. GALLOT

ONERA, FRANCE
AEROSPATIALE, FRANCE

September 7-9, 1977
AIX-EN-PROVENCE, FRANCE

ASSOCIATION AERONAUTIQUE ET ASTRONAUTIQUE DE FRANCE

## INTRODUCTION

The research for new airfoils has become essential to follow the helicopter technological improvements realized on the structure transmission assemblies and engines. A big effort made by AEROSPATIALE in this field has been materialized by practical achievements on the PUMA SA 330. The improvement resulting from the adoption of composite blades for which a new family of airfoils is used, is shown on figure 1.

In addition, due to the improvements realized by the airfoil design methods developed particularly by ONERA and AEROSPATIALE, it is possible today to predict more accurately the aerodynamic characteristics of a new airfoil.

The study of a new generation of helicopter blade airfoils has been started by ONERA at the request of AEROSPATIALE who stated the design objectives based on their knowledge of the rotor aerodynamic flow environment. Therefore, the first part of this lecture describes how the first airfoil of this family : OA 209 was generated. The second part gives some indications on the gains anticipated on the rotor with this new airfoil and the first results obtained in flight on the "Dauphin " SA 360 helicopter.

## 1. DESIGN OBJECTIVES FOR HELICOPTER ROTOR AIRFOIL

The drawing-up of design objectives for rotor airfoil requires a good knowledge of the rotor aerodynamic flow environment (and even aeroelastic behaviour in some cases), the detailed analysis of the missions to be performed by the helicopter under consideration, knowing the limitations of the design methods applicable to airfoil in bi-dimensional airflow, and the test facilities in steady and unsteady conditions.

As to the first point, the methods developed by ONERA as well as by AEROSPATIALE (ref. 1, 2, 3) describe rather accurately the aerodynamic (and aeroelastic) behaviour of the rotor as long as the latter does not include excessively stalled areas or is not subjected to highly unsteady compressible phenomena at the blade tip.
The model rotor experimentation in the large S1 Modane wind tunnel made it possible to obtain all the data on the blade load variation necessary to test these theoretical prediction tools (ref. 4 and 5).

As far as the second point is concerned, our helicopters have been, so far, designed as multi-purpose aircraft, used both for military and civil operations. It is why, we attached a great importance to the increase of manoeuvrability and payload (increase of the maximum weight, reduction of the fuel consumption in cruising flight) and to the improvement of hover performance in altitude.

Finally, as to the last point, the design objectives must be adapted to the capabilities of prediction tools in the aerodynamic airfoil performance field. For this reason, the unsteady criteria are eliminated and replaced by equivalent steady criteria ($C_L$ max., $M_D$, Mach tuck etc...).

The examination of figure 2 shows the stringent nature of the requirements for an airfoil or a helicopter blade outboard section (0.75 R - 0.9 R)

- High $C_L$ max for M = 0.3 - 0.4
- High $M_D$ for $C_L \leqslant 0.1$ with a low $C_D$ level

In addition, the selected airfoil must have a low drag coefficient for M = 0.6, $C_L$ = 0.6 both in cruising flight (front and rear blade) and in hover flight (more especially when the rotor is heavily loaded).

With the advent of the composite blade technology (fibreglass or carbon) the aerodynamicist can select an evolutive geometry and adapt the airfoil, at the best, to the considered blade spanwise section. So, one obtains the definition of an airfoil family, the technical specifications of which are derived from those of the main section but with more stringent requirements for one of the above points, taking into consideration the differences of local Mach or CL required (see fig. 2).

In our case, the airfoil NACA 0012 being taken as reference, the following points have been retained as requirements :

. Hover and level flight in altitude

To reduce the airfoil power absorbed by the rotor, the airfoil lift-to-drag ratio shall be improved by 20 to 30 per cent for ($C_L$ = 0.6 - M = 0.6). In addition, the $C_L$ level for which the drag increases rapidly, must be increased by 0.2 to reduce the interference effect on the following blade generated by the previous blade tip vortex in hovering flight.

. Advancing blade operation

It is necessary to extend the drag divergence Mach number at near zero lift coefficient in order to reduce the important drag due to the advancing blade on fast aircraft, or to allow simultaneously a chord reduction and an increase of rotor r.p.m. on a slower aircraft.

A gain of 0.05 Mach is to be aimed at, maintaining a comparable level of $C_D$ before the divergence and a moderate increase of $C_D$ beyond ($C_D$ = 0.012 for $C_L$ = 0 at M = 0.85).

. Retreating blade operation

The rotor limits, especially in manoeuvres or in altitude are connected to $C_L$ max for Mach values between 0.3 and 0.4. An increase of $C_L$ max by 0.3 is recommended to increase the maximum capabilities of the rotor.

. Requirements on moments

Contrary to other manufacturers (ref. 6, 7, 8) we have stringent requirements for the value of Cmo since we have $|Cmo| \leqslant 0.005$. We feel that for relatively flexible blades, the torsion effect induced by a high Cmo would be prejudiciable, associated with a pitch link load increase which would penalize the control rods from the service life aspect.

In addition, as far as our light aircraft are concerned, the increase of the pitch link loads is detrimental in the "servo-off" mode and reduces the flight envelope with load factor, usually limited by the jack stall. Therefore, the value $|Cmo| < 0.005$ is considered as desirable and $|Cmo| < 0.01$ as essential for Mach numbers between 0.6 and 0.8. In addition, "Mach-tuck" associated with the building-up of important shock waves on an airfoil should occur after the drag divergence Mach number.

. Technological constraints

To obtain a sufficient torsional stiffness and a satisfying structural strength, the relative thickness has been fixed to 10 % $\pm$ 1 %. Moreover, a 5 % trailing edge strip has been included in the definition; this strip facilitates the bonding of the trailing edge and allows a possible adjustment of Cmo.

## 2. ROTOR AIRFOIL DESIGN

### 2.1. Introduction

The aim for this airfoil design was to improve the performance of the conventional profiles, such as NACA 0012, in the three primary areas of interest for a helicopter main rotor blade, i.e. manoeuvres, hover and high speed advancing blade. However the main objective was to design an airfoil which was well-adapted to hover and high speed.

Table 1 presents the design objections for this airfoil in the different flight areas

Table 1. Airfoil design objections

| Flight condition | Quantity | Design objections |
|---|---|---|
| Hover | $C_L/C_D$ for $M = 0.6$ $C_L = 0.6$ | 72 |
| | $C_L$ for $M_{DD} = 0.6$ | 0.9 |
| High speed | $M_{DD}$ at $C_L \sim 0$ | 0.85 |
| | $\lvert Cmo \rvert$ | $\leq 0.01$ |
| Manoeuvres | $C_L$ max at $M = 0.4$ | 1.4 |
| | $C_L$ max at $M = 0.5$ | 1.3 |

Two methods can be used to design an airfoil : direct or inverse.

The direct methods were mainly used until a few years ago. The idea is to modify the geometry of a well-known airfoil in order to improve the performance for a particular flight condition.

The basic rules used for changing the shape are deduced from the test analysis of the NACA series profiles or from studies of the influence on the airfoil performance of individual variations in airfoil geometric parameters (thickness ratio, camber... (ref. 9, 10).

Table II gives examples of airfoils obtained by modification of some NACA series.

Table II - Examples of airfoils designed by direct methods

| NACA Series | Airfoils |
|---|---|
| NACA 00XX | NPL 9615, 9626, 9627, 9660, "ONERA NACA cambré" |
| NACA 130XX | V 13006 - 0,7 |
| NACA 131XX | SA 13109-1,58 - SA 13106-0,7 |
| NACA 230XX | V 23010-1,58 |
| NACA 6 X series | VR5 - VR7 - VR8 - VR9 - HH01 HH02 |

More details on the shapes and performance of these airfoils can be found in the ref. 11 to 17.

The main defect of the direct methods is that the improvement of the quality of an airfoil for a particular point (e.g. max) is usually accompanied by a deterioration of other characteristics (e.g. Cmo).

The progress in fixed wing airfoil design methods made these last years brought to light new processes, including inverse methods, which are a great improvement over the direct methods (18).

Hodograph techniques are described in (19, 20, 21) while ONERA and AEROSPATIALE prefer purely inverse methods (22, 23) where the prescribed velocity distribution on the airfoil is the input and permits a direct control of the aerodynamic coefficients($C_L$, $C_D$, Cm).

## 2.2. Airfoil design and performance

The different steps of the design process are :

- the choice of a prescribed velocity distribution
- the calculation of the airfoil shape
- the theoretical evaluation of the performance for all flight conditions.

After these three steps, an experimental control is necessary, because the theoretical calculations are not able at the time to predict with a high degree of accuracy some aerodynamic coefficients, like the $C_L$ max or the MDD.

The choice of the velocity distribution has been made at $C_L \sim 0.6$

The different steps in this choice and the consequences on the performance and on the shape of the airfoil are described on figure 3.

- To obtain an improvement of $C_L/C_D$ at M = 0.6 and $C_L$ = 0.6, the upper surface velocity distribution has been chosen to have a constant level near M = 1 for M = 0.6 on the first 18 per cent, followed by a compression law deduced from boundary layer computations. To maintain the level of lift, the lower surface velocity distribution differs also near the leading edge from those of a conventional airfoil (fig. 3a).
  This velocity distribution leads to a leading edge camber and to a nose-down zero lift pitching moment.

- To reduce the Cmo, the lower surface velocity distribution is modified so as to increase the load in the first 25 per cent of the chord.
  The thickness of the leading edge decreases, with a possible deterioration of the performance for the low lift coefficient in high speed flight. The thickness ratio decreases also (Fig. 3b).

- To have the thickness ratio required, a modification of the velocity distribution due to the thickness effect is made with a higher level on the aft part of the chord and a peaky effect near 30 % to reduce the velocity at the crest (Fig. 3c).

The airfoil computed from this velocity distribution has been called OA1. Its contour is also drawn on figure 3.

The performance of the OA1 airfoil has been estimated in all flight conditions with a transonic viscous code described (ref. 24).
The results indicated that the main objectives of table I could be reached with, however, a risk of boundary layer separation on the lower surface near the leading edge for low lift coefficients.

This airfoil has been tested in two-dimensional steady flow in the ONERA S3 Modane wind tunnel. The global performance plotted on Figure 4, shows that for the $C_L$ max at $M \leqslant 0.5$ and for the $M_{DD}$ at low $C_L$ the improvements, compared to the NACA 0012 airfoil, are important. However the drag level at $C_L \sim 0$ and the Cmo are greater than expected (fig. 5). This is due to a laminar boundary layer separation on the lower surface near the leading edge, which can be seen on the pressure distributions for several Reynolds numbers (Fig. 6). So it was decided to modify the airfoil to avoid this defect.

The modification of the zero lift velocity distribution is shown on figure 7. It consists of a lower surface peak level reduction and a new velocity distribution on the aft part of the airfoil, to keep a low Cmo. A trailing edge tab has also been included in the design.

The airfoil obtained by the inverse computation from this new velocity distribution has been called OA 209. It was also tested in the ONERA S3 Modane wind tunnel. Its performance is shown on Figures 8 and 9 in terms of $C_L$ max at $M \leqslant 0.5$, $M_{DD}$ at constant $C_L$ for $M > 0.5$ and Cmo.

The objectives of table I have been reached for the $M_{DD}$ at $C_L = 0$, which is 0.85 and for the Cmo which is very low, even for high Mach numbers. For hover conditions, the $C_L/C_D$ at $M = 0.6$ and $C_L = 0.6$ is .75, and $M_{DD} = 0.6$ for $C_L = 0.8$.

For manoeuvring flight, the $C_L$ max is 1.27 at $M = 0.3$ and 1.21 at $M = 0.4$. These values of $C_L$ max are lower than those at the objectives, but remain important for a nine per cent thick airfoil.

## 2.3. Comparison with other airfoil characteristics

It is always difficult to compare results of airfoils tests which have been made in different wind tunnels and for various Reynolds numbers. However, if the aerodynamic coefficients can be affected by the test conditions, they provide a reasonable basis for comparison and discussion.

Figure 10 shows the contours of the airfoils selected for this comparison. It includes airfoils of about the same thickness ratio than the OA 209 and whose test results are published.

The comparison includes also the NACA 0012 because it was the basic profile for the design and it has been tested in the same conditions and in the same wind tunnel as the OA 209.

These airfoils are :

- NACA profiles : NACA 0012 - NACA 63 A 009 - NACA 64 A 608.

- profiles designed by Boeing Vertol from NACA series V (1.9) 3009-1.25 , V23010-1.58 with a 3° trailing edge tab. VR8 with 0° trailing edge tab.

- profiles designed by Dr. Wortman : FX 69H - 098
  FX 69H - 090

The values of the aerodynamic coefficients for these airfoils have been found in ref. 16 and 18.

Figure 11 compares some of the main sectional characteristics for the different flight areas, which are :

- $C_L$ max at M = 0.4 and 0.5
- Cmo
- drag divergence Mach number $M_{DD}$ at CL ∿ 0
- drag coefficient at M = 0.6 and $C_L$ = 0.6

- The symmetrical NACA airfoils have poor maximum lift capability while the cambered 64 A 608 has high $C_L$ max and a low drag level at M = 0.6, but an unacceptable Cmo.

- The V(1.9) 3009 - 1.25 has relatively good characteristics in all the flight areas but a relatively high Cmo. A trailing edge tab for a zero lift pitching moment compensation will decrease the $C_L$ max by about 0.1.

- The V23010-1.58 with a 3° TE tab has a high $C_L$ max at M = 0.4 but not at M = 0.5 and the hover characteristics are poor.

- The VR8 with a 0° TE Tab gives some improvements on the V23020-1.58 in hover and forward flight, but a tab deflection for Cmo compensation will cause deterioration of its performance in manoeuvres.

- The FX 69H-098 and FX 69H-090, designed by Dr. Wortman, have a very good performance in hover but not for $M_{DD}$ and the Cmo is quite important.

- The OA209 airfoil gives a good compromise for all the flight areas. It has a high $M_{DD}$ and a very low Cmo. Its performance in hover and manoeuver is about the same as those of the other profiles, especially if we take into account the decrease of $C_L$ max due to a zero lift pitching moment compensation for the other airfoils.

Figure 12 from ref. 16, compares the characteristics of some airfoils on the basis of their maximum lift capability at M = 0.4 and 0.5 and the drag rise after drag divergence which is defined by the Mach number where the zero lift drag reaches a value of $C_{DO} = 0.018$. The comparison is also made on figure 12 on the basis of the Mach tuck - Mach drag divergence diagram for several rotor configurations and sections at 90 per cent span station.

Figure 12 outlines the good compromise realised with the OA 209 airfoil ; this constitutes a basic profile for the design of a family of rotor blade sections with a thicker section for inboard stations on the blade and a thinner section for the tip, it will be possible to design a blade with very high performance in all the flight areas.

## 2.4. Comparison with theoretical predictions

The theoretical evaluation of the performance of an airfoil needs transonic viscous computer codes and it is necessary to know with which degree of accuracy the evaluations are made.

The computer code used by AEROSPATIALE and ONERA is described (ref. 24). It uses the Garabedian and Korn method for the non-viscous transonic flow analysis. The viscous effects are taken into account by the boundary layer displacement thickness added on the profile and computed by an integral method developed at ONERA.

Figures 13 a, b, c show comparisons at M = 0.3 - 0.5, 0.6 between the S3 Modane tests and the calculations. For each mach number the curves $C_L - \alpha$, $C_L - C_D$, $C_L - Cm$ have been plotted. The agreement is good for all the aerodynamic coefficients, even for high lift coefficients. It can be outlined also that the pitching moment of the airfoil is always very low and that the aerodynamic center is about at 25 % of the chord.

However this computer code is unable to compute configurations with boundary layer separation, so the $C_L$ max cannot be predicted with accuracy.

Figure 14 shows comparisons in terms of drag coefficient versus Mach number for three levels of lift : $C_L = -0.1$, $C_L = 0$, $C_L = 0.1$.

The agreement is generally good but some discrepencies appear at high Mach number. The shock positions at the same levels of lift are also well-predicted (fig. 15).

For the zero lift pitching moment coefficient Cmo (fig. 16), the theoretical evaluation gives values quite different from those of experiments for high Mach numbers due to differences of the pressure distribution on the aft part of the airfoil.

These comparisons between theory and experiment are generally good. So the combination of this direct code with the inverse one for the airfoil design are very efficient and useful tools for the aerodynamicist.

## 3. IMPROVEMENTS ANTICIPATED WITH THE OA 209 AIRFOIL

Considering the compressible bi-dimensional results obtained in the S3 Modane wind tunnel, the analysis of the gains to be obtained with the OA 209 airfoil, has been made, using the simplified performance calculation method described in Ref. 3.

The examination of Figure 17 shows that the use of the OA 209 airfoil enables the increase by about 10 % of the rotor lift level which corresponds to a maximum lift-to-drag ratio, and the stall limit inception by 5 %. Of course, these important gains are due to a lower drag level in the retreating blade disc area and to the increase of $C_L$ max.

The application to an aircraft, like the Dauphin SA 360, makes it possible to anticipate the following gains.

- Hovering flight : the improvement obtained in the area M = 0.6, $C_L$ = 0.6 should allow a gain in take-off weight, at constant power, varying from 2 to 5 % according to the rotor-load level.

- Forward flight : the gain in power is 7 % in cruising flight at sea level and 12 % at 2000 m ; this is due to the increase of the drag divergence Mach number at a low $C_L$ and to the drag improvement on the front and rear blade near the stall limit in altitude. In addition, the load level can be increased by 5 to 10 % taking into account the increase of the lift level permissible in forward flight as calculated above.

In order to evaluate these gains, an experimentation has been made on a model rotor in the large S1 Modane wind tunnel. The two model rotors used were four bladed rotors having a 4 m diameter, 140 mm chord, and rotating at a tip speed of 210 m/s. The simulation made it possible to cover advance ratios from $\Lambda$ = 0,2 to $\Lambda$ = 0.5 corresponding easily to the actual helicopter flight envelope. The blades of the rotor No 5 which was used as reference, were generated with NACA 0012, SA 13109 BA1.58 and SA 13106-0.7 airfoils ; the rotor No 6 blades were generated with the OA 209 airfoil.

As the SA 13109 BA 1.58 airfoil has characteristics similar to those of the NACA 0012 (ref. 15) as far as $C_L$ max and drag level at M = 0.6 and $C_L$ = 0.6 are concerned, the comparison can be made only for conventional advance ratios in which the drag divergence Mach number influence is not significative.
Both rotors were successfully experimented at $\Lambda$ = 0.5 up to M = 0.92 at the advancing blade tip, rotor 5 behaved better at high Mach number considering its lower thickness ratio at the blade tip.

Results mentioned on Figures 18 and 19 show clearly the improvement of the lift-to-drag ratio anticipated for high loads usually used on helicopter in altitude. This gain is maintained within the range of usual advance ratios ($\Lambda$ = 0.2 to 0.4).

## 4. EXPERIMENTATION IN FLIGHT (Full scale)

In order to compare more directly and to check the gains on a full scale rotor, a set of experimental blade with a OA 209 constant airfoil was built for the SA 360 Dauphin. An experimentation in flight took place recently ; it enabled the comparison between the behaviour of the conventional rotor (NACA 0012) and that of the experimental rotor. Tests were performed on an aircraft flying in overload conditions with respect to the maximum weight of Dauphin.

Although the experimentation was made partially, results were deemed very interesting. On the one hand the flight envelope in forward flight was largely increased, as shown on figure 20 where are grouped all test points obtained at maximum engine power for both rotors. The gain in weight is approximately of 10 % whatever the speed is. Figure 21 shows the gain in speed at constant power ; this speed gain varies from 5 km/h to 50 km/h between sea level and 4000 metres. Considering the small number of test points, we tried to sum up the power gains obtained with the blades OA2 in the shape of the diagram "average CD vs $CT/\sigma$" (Fig. 22). This diagram shows the improvement brought by the rotor OA 209 especially at high load ($CT/\sigma > 0.07$).

As far as hover performance is concerned, the test points performed in OGE hover have shown a gain in take-off weight of 2 %. Therefore, it is to be expected that this gain will be higher in altitude.

No abnormal feature was evidenced in the pitch link alternating loads, this is in accordance with the low value of the airfoil Cmo.
The analysis of the fixed servo static loads showed a substantial reduction of the lateral stick force, which allows a larger flight envelope in the case of a light helicopter when a hydraulic failure occurs (fig. 23).

The vibration level has been considered as being much better with the set of blades "OA 209" in forward flight in altitude and with a load factor (fig. 24), although the aircraft flew in overload conditions. This result is logical since the vibration level of a helicopter is usually affected when the rotor lift-to-drag ratio starts to decrease at high advance ratio or high loading.

The conclusion of these partial tests can be summarized by the pilot's opinion : the change of airfoil should allow an increase of the aircraft weight by at least 10 % with a flight envelope identical to that of the conventional rotor, without affecting the comfort and the margins of the aircraft.

## CONCLUSION

The various tests carried out on the OA 209 airfoil both in wind tunnel and in flight lead to the following conclusions :

- The viscous transonic airflow computer codes used by ONERA and AEROSPATIALE give a correct estimate of the airfoil performance in steady airflow.

- The OA 209 airfoil performance in steady airflow is definetely more important than that of the conventional airfoils. If compared to other new airfoils, presently known, this airfoil is considered as being a good compromise between all the requirements relative to a section located at 75 - 90 % of the span.

- The gains expected by the user of this airfoil on an actual blade have been confirmed by flight tests :

  . increase of the lift-to-drag ratio in hover

  . increase of the flight envelope

  . reduction of the vibration level and of pitch link loads.

- The use of airfoils derived from OA 209 airfoil for the production of an evolutive blade should allow still more important gains in the complete flight envelope.

## REFERENCES


1. R. DAT

Applications des méthodes linéaires à l'étude du comportement aéroélastique des hélicoptères.
13ème congrès international de mécanique théorique et appliquée.
Moscou 1972

2. J.J. COSTES

Rotor response prediction with non-linear aerodynamic loads on the retreating blade.
2nd European rotorcraft and powered lift aircraft forum
Bückeburg 1976

3. J. GALLOT

Calcul des charges sur rotor d'hélicoptère
Helicopter rotor loads prediction methods
AGARD CP No 122. 1973

4. M. LECARME

Comportement d'un rotor au-delà du domaine de vol usuel à la grande soufflerie de Modane.
AGARD conférence Proceedings No 112 (1972)

5. M. LECARME

Comportement d'un rotor au-delà du domaine usuel à la grande soufflerie S1 de Modane Avrieux. AGARD CP No 111 (1973)

6. L. LADONE, T. FUKUSHIMA

A review of design objectives for advanced helicopter rotor airfoils
A.H.S. Symposium (1975)

7. V.M. PAGLINO and D.R. CLARK

A study of the potential benefits of advanced airfoils for helicopter applications.
A.H.S. Hartford - March 1975

8. G. REICHERT, S.N. WAGNER

Some aspects of the design of rotor airfoil shapes
AGARD Conference Proceedings No 111 (1973)

9. R.W. PROUTY

A state-of-the-Art survey of two dimensional airfoil data
A.H.S. on helicopter aerodynamic efficiency (1975)

10. G.J. BINGHAM

An analytical evaluation of airfoil sections for helicopter rotor applications.
NASA TND 7796 February 1975

11. GREGORY N., WIBY P.G.

NPL 9615 and NACA 0012 - A comparison of aerodynamic data
ARC CP No 1261 1973

12. WILBY P.G., GREGORY N. and QUINCEY V.G.

Aerodynamic characteristics of NPL 9629 and NPL 9627. Further airfoils designed for helicopter rotor use.
ARC. CP No 1269 - November 1969

13. WILBY P.G.

Effect on production modifications to the rear of Westland Lynx Rotor blade on sectional aerodynamic characteristics.
RAE TR 73043 February 1973

14 P. FABRE

Problèmes de traînée des appareils à voilures tournantes.
AGARD Lectures Series No LS/63

15. J. RENAUD and F. NIBELLE

Effects of the airfoil choice on rotor aerodynamic behaviour in forward flight.
2nd European rotorcraft and powered lift aircraft forum
September 20-22 1976 Bückeburg.

16 L. DADONE - T. FUKUSHIMA

A review of design objectives for advanced helicopter rotor airfoils.
A.H.S. 1975

17. KENNET B. AMER, Sally V. LA FORGE, JAMES R. NEFF and RAY W.PROUTY

Aerodynamic and dynamic design and development of the main rotor of the YAH-64 advanced attack helicopter.
A.H.S. 1976

18. J.W. SLOOF - Fx. WORTMAN - J.M. DUHON

The development of transonic airfoils for helicopters
A.H.S. 1975

19. BAUER F., GARABEDIAN P. and KORN D.

Supercritical wing sections
Springer Berlin 1972 No 66

20. F. BAUER - P. GARABEDIAN - D. KORN and A. JAMESON

Supercritical wing sections II
Springer Berlin 1975

21. BOERSTEL J.W. and HUIZING G.H.

Transonic shock free airfoil design by an analytical hodograph method.
AIAA paper 74-539 (1974)

22. Y. MORCHOISNE

Méthode inverse de détermination des profils en incompressible
AAAF 11ème colloque d'aérodynamique appliquée (1974)

23. Y. MORCHOISNE

Méthode de calcul inverse en écoulement compressible
AAAF 12ème colloque d'aéro dynamique appliquée (1975)

24. J. BOUSQUET

Calculs bidimensionnels transsoniques avec couche limite
11ème colloque AAAF 1974

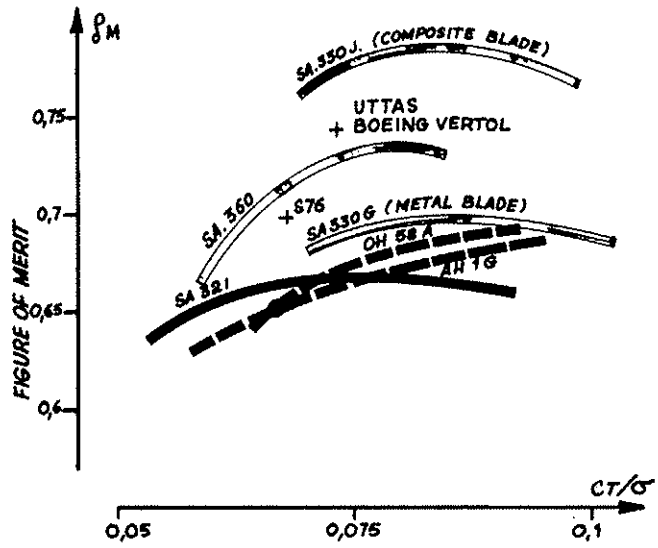


FIG.1 IMPROVEMENT OF ROTOR EFFICIENCY

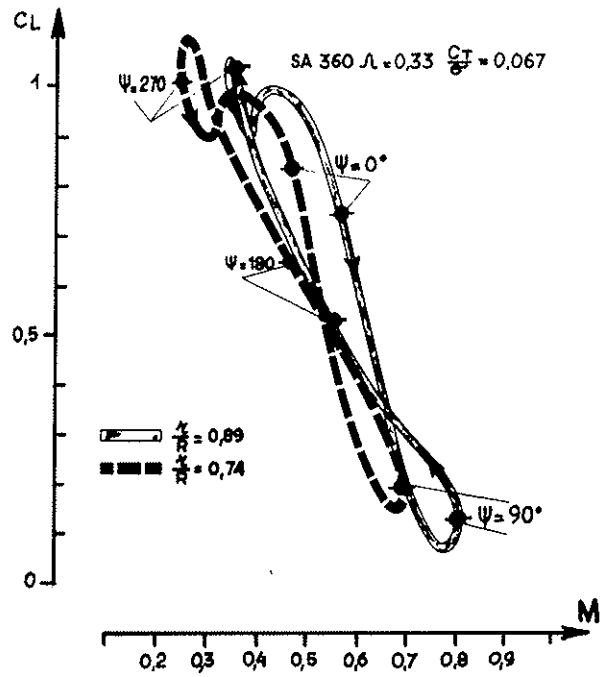


FIG.2 AIRFOILS OPERATING RANGE

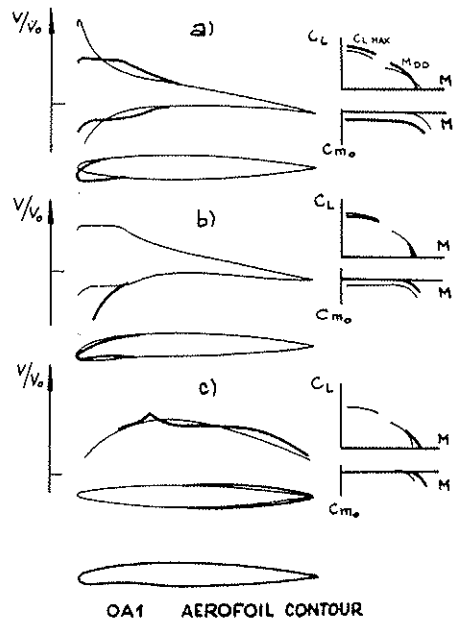


FIG.3 DESIGN OF THE OA1 AIRFOIL

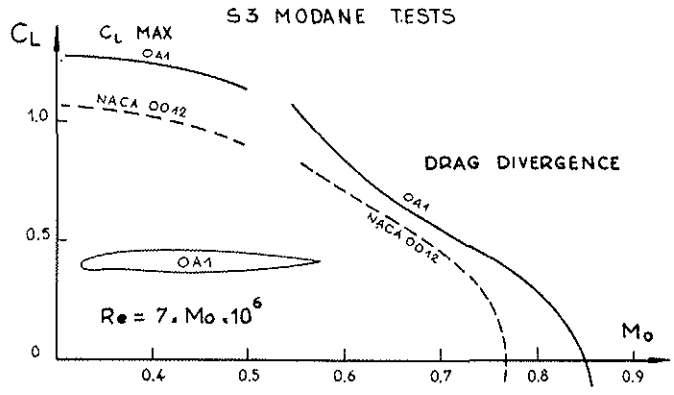


FIG.4 OA1 GLOBAL PERFORMANCE

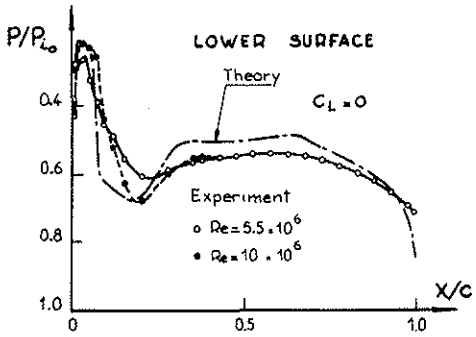


FIG.6 OA1 LOWER SURFACE PRESSURE DISTRIBUTION $C_L \sim 0$ $M_0 = 0.8$

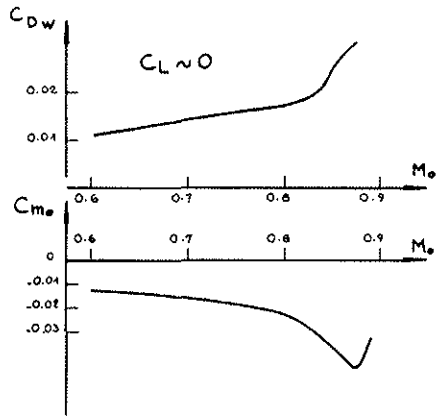


FIG.5 OA1 TEST RESULTS

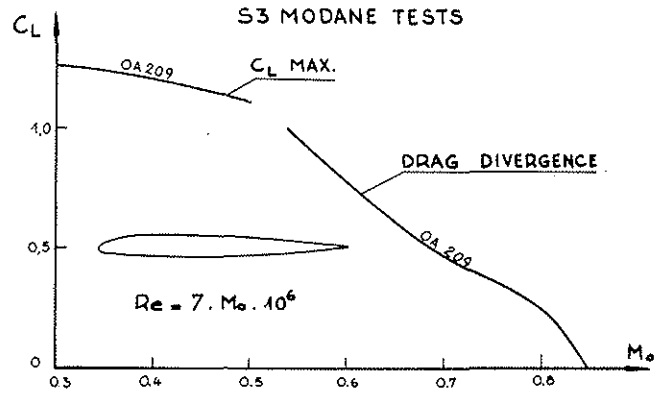


FIG. 8 OA 209 GLOBAL PERFORMANCE

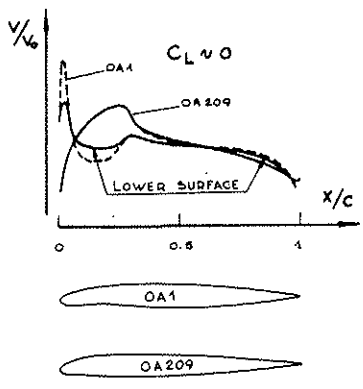


FIG.7 OA 209 AIRFOIL DESIGN

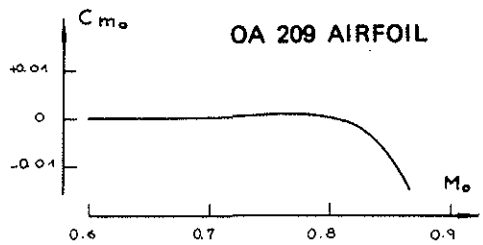


FIG.9 ZERO LIFT PITCHING MOMENT COEFFICIENT

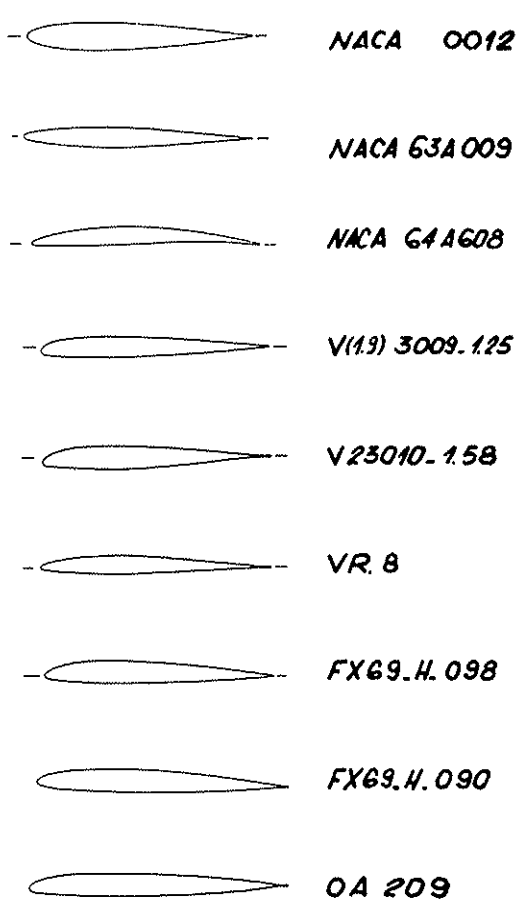


FIG.10 COMPARISON OF AIRFOILS

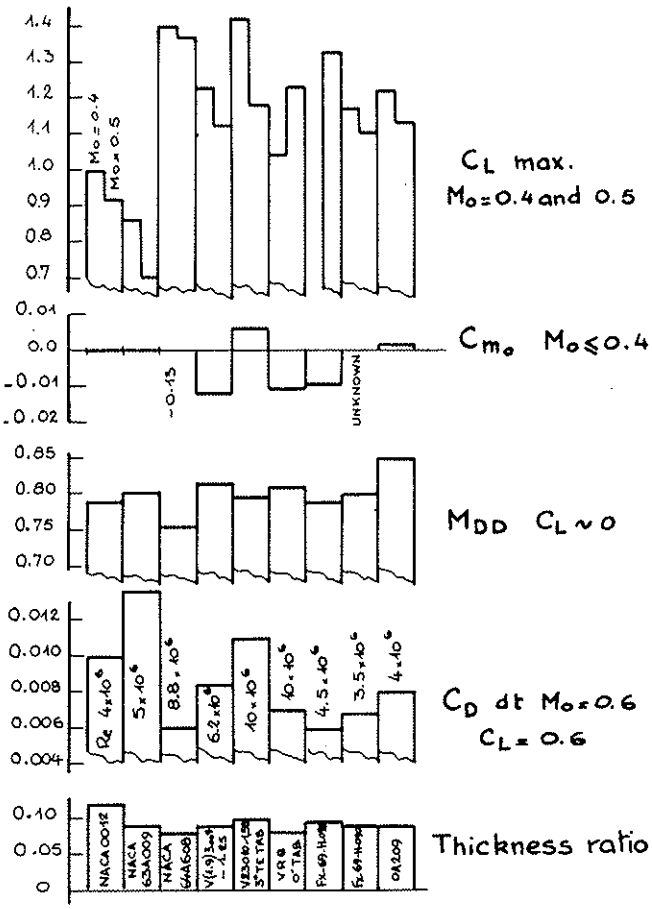


FIG.11 COMPARISON OF SECTIONAL CHARACTERISTICS

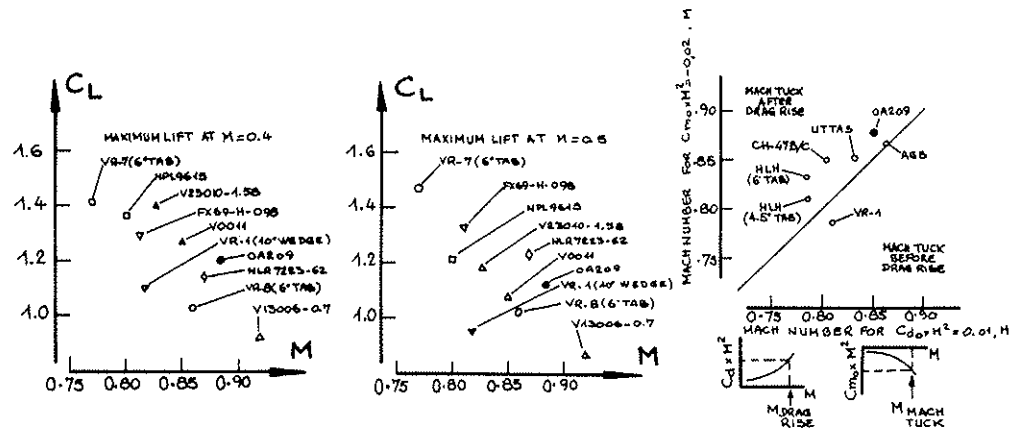


FIG.12 COMPARISON OF SEVERAL HELICOPTER ROTOR AIRFOIL SECTIONS

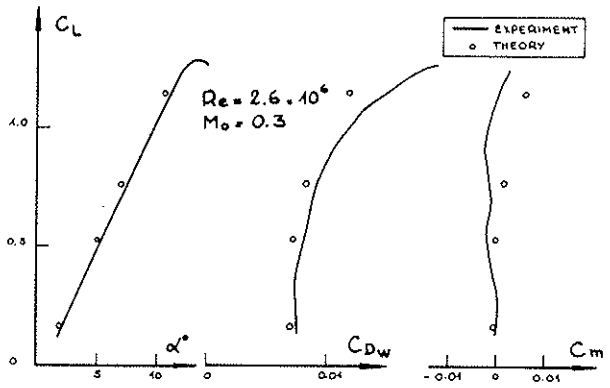


FIG.13a

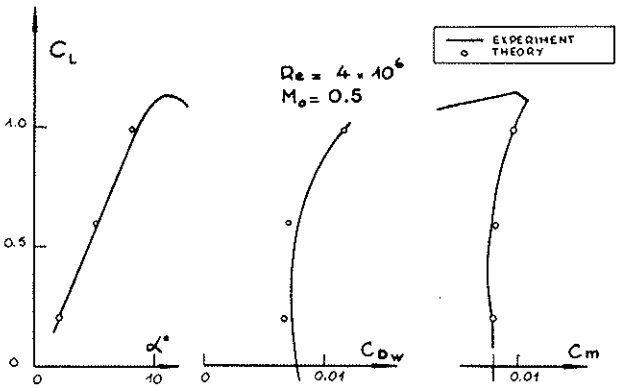


FIG.13b

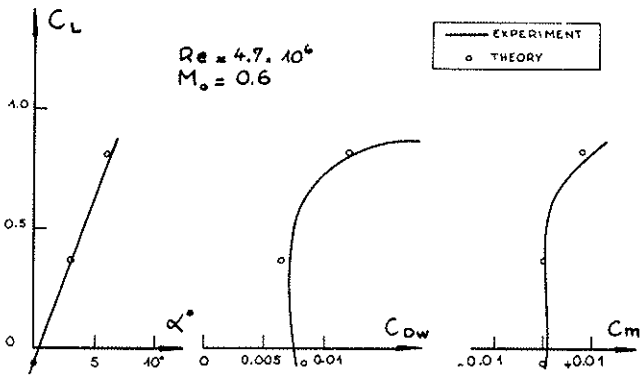


FIG.13c

FIG.13 OA 209 AIRFOIL COMPARISON BETWEEN THEORY AND EXPERIMENT

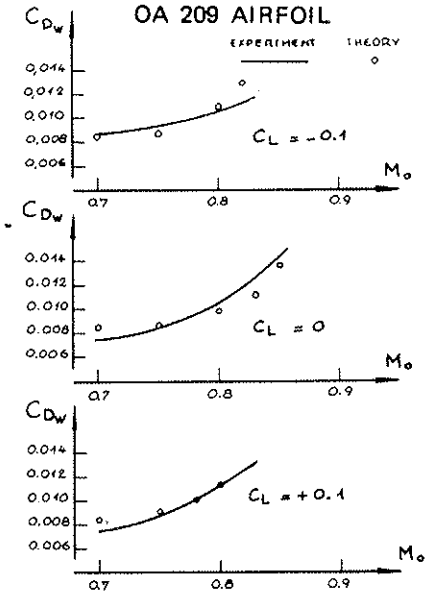


FIG.14 EVOLUTION OF THE THEORETICAL AND EXPERIMENTAL DRAG COEFFICIENT

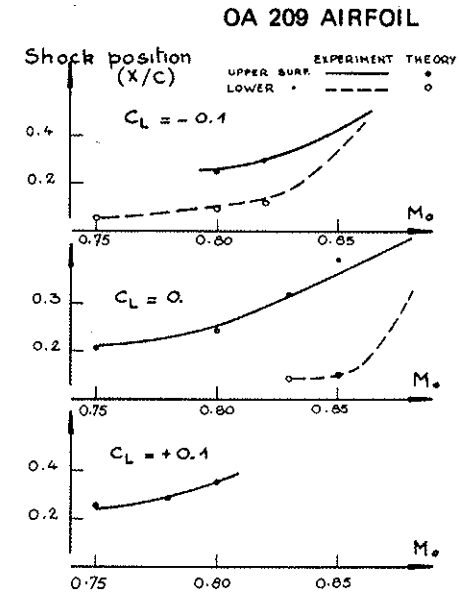


FIG.15 EVOLUTION OF THE THEORETICAL AND EXPERIMENTAL SHOCKS POSITIONS

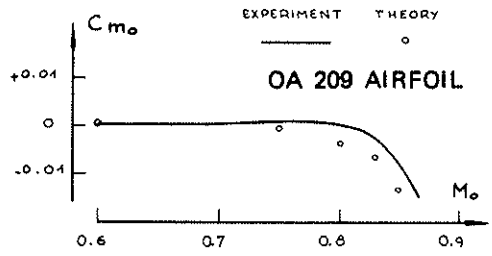


FIG. 16 EVOLUTION OF THE THEORETICAL AND EXPERIMENTAL ZERO LIFT PITCHING MOMENT COEFFICIENT

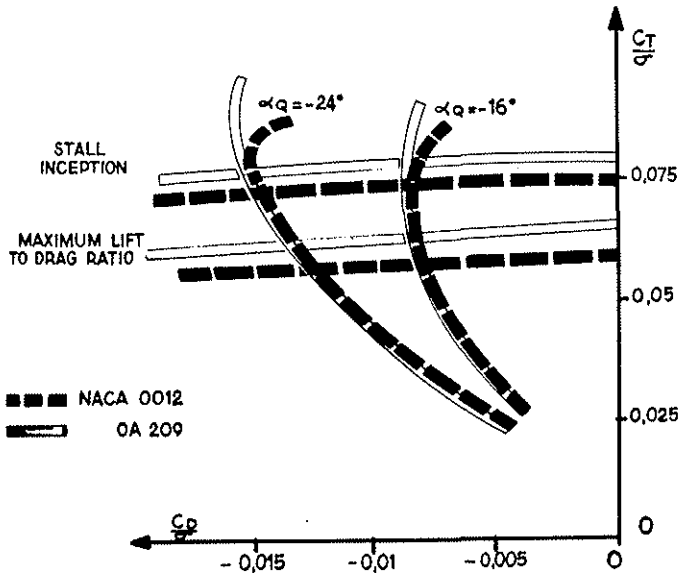


FIG. 17 AIRFOIL INFLUENCE ON ROTOR LIMITS
MODANE MODEL ROTOR $\mu$=0.4

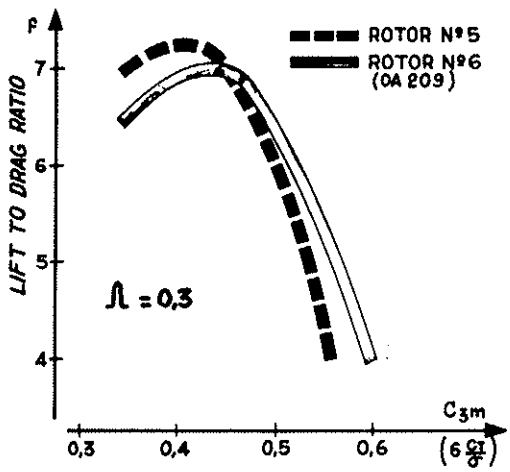


FIG.18 LIFT TO DRAG RATIO INCREASE
FOR HIGH LOADED ROTOR

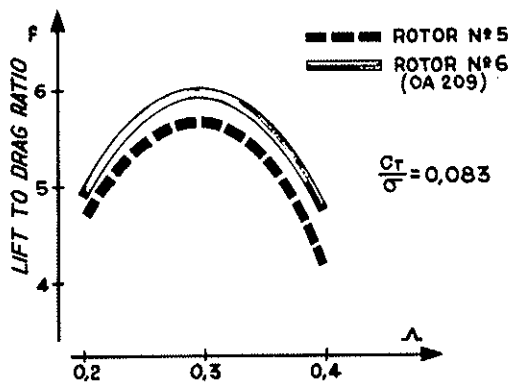


FIG.19 ADVANCE RATIO INFLUENCE ON
LIFT TO DRAG RATIO

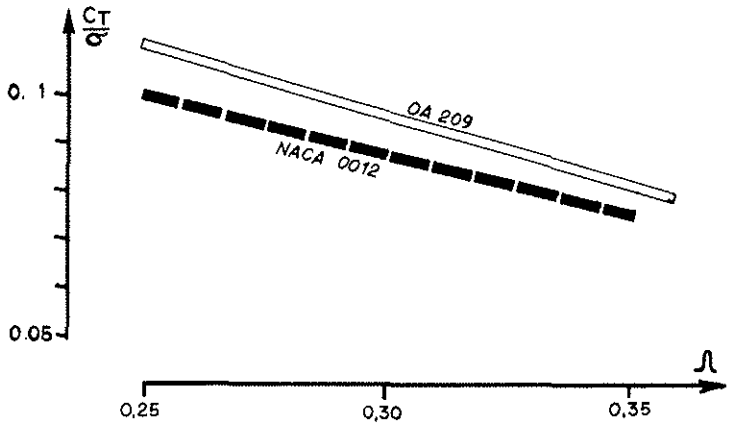


FIG.20 INCREASE OF LEVEL FLIGHT ENVELOP

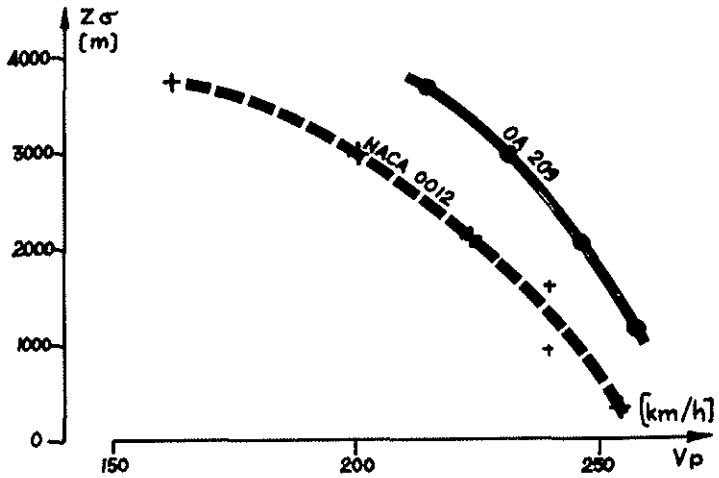


FIG.21 AIRFOIL INFLUENCE ON MAXIMUM LEVEL SPEED

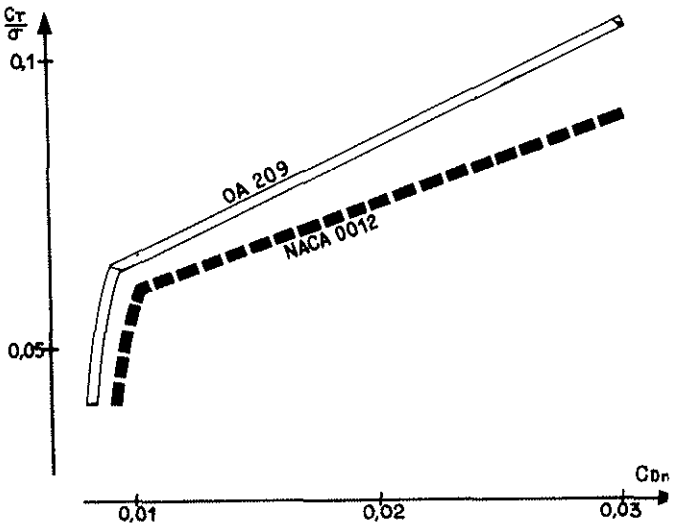


FIG.22 SYNTHESIS OF GAINS OBTAINED WITH OA 209 AIRFOIL IN LEVEL FLIGHT

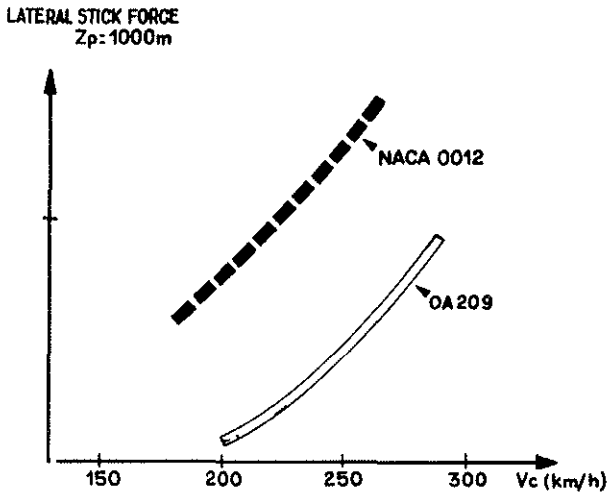


FIG.23 AIRFOIL INFLUENCE ON LATERAL STICK FORCE

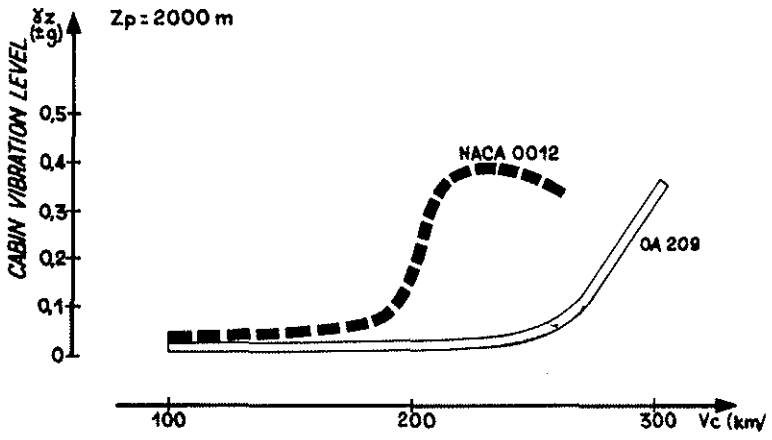


FIG.24 AIRFOIL INFLUENCE ON VIBRATION LEVEL FOR HIGH LOADED ROTOR